



Quantitative Analysis of Seeing with Height and Time at Muztagh-Ata Site Based on ERA5 Database

Xiao-Qi Wu^{1,2} , Cun-Ying Xiao^{1,2,*} , Ali Esamdin^{3,4}, Jing Xu^{3,4}, Ze-Wei Wang^{1,2}, and Luo Xiao^{1,2}
¹ Institute for Frontiers in Astronomy and Astrophysics, Beijing Normal University, Beijing 102206, China; xiaocunying@bnu.edu.cn
² Department of Astronomy, Beijing Normal University, Beijing 100875, China
³ Xinjiang Astronomical Observatory, Chinese Academy of Sciences, Urumqi 830011, China
⁴ University of Chinese Academy of Sciences, Beijing 100049, China

Received 2023 August 4; revised 2023 September 28; accepted 2023 October 18; published 2023 December 13

Abstract

Seeing is an important index to evaluate the quality of an astronomical site. To estimate seeing at the Muztagh-Ata site with height and time quantitatively, the European Centre for Medium-Range Weather Forecasts reanalysis database (ERA5) is used. Seeing calculated from ERA5 is compared consistently with the Differential Image Motion Monitor seeing at the height of 12 m. Results show that seeing decays exponentially with height at the Muztagh-Ata site. Seeing decays the fastest in fall in 2021 and most slowly with height in summer. The seeing condition is better in fall than in summer. The median value of seeing at 12 m is 0.89 arcsec, the maximum value is 1.21 arcsec in August and the minimum is 0.66 arcsec in October. The median value of seeing at 12 m is 0.72 arcsec in the nighttime and 1.08 arcsec in the daytime. Seeing is a combination of annual and about biannual variations with the same phase as temperature and wind speed indicating that seeing variation with time is influenced by temperature and wind speed. The Richardson number Ri is used to analyze the atmospheric stability and the variations of seeing are consistent with Ri between layers. These quantitative results can provide an important reference for a telescopic observation strategy.

Key words: site testing – atmospheric effects – methods: data analysis – telescopes – Earth

1. Introduction

The search for high-quality observatory sites has become an important factor in the development of astronomical research. The site testing works carried out at the South Pole, Dome A, and Dome C have revealed the advantages of a strong but thin boundary layer, high atmospheric transmittance, and good seeing in the Antarctic region (Zhou et al. 2010; Aristidi et al. 2015; Shi et al. 2016). A site testing campaign was initiated from 2016 to 2019 among three sites: Ali in Tibet, Daocheng in Sichuan, and Muztagh-Ata in Xinjiang (Feng et al. 2020). In 2017, Xinjiang Astronomical Observatory started monitoring the Muztagh-Ata site (Xu et al. 2020a, 2020b). The site is located on the eastern part of the Pamir Plateau, in the southwest of Xinjiang Uygur Autonomous Region of China whose geographical location is $38^{\circ}19'46''$ N, $74^{\circ}53'48''$ E with an altitude of 4526 M above sea level. The Muztagh-Ata One-point-nine-three-meter Synergy Telescope (MOST) constructed by Beijing Normal University, Xinjiang Astronomical Observatory, and Xinjiang University is going to be placed at the Muztagh-Ata site.

Seeing is the most essential parameter to evaluate the quality of astronomical sites. Seeing is defined as the clarity of the image displayed by a telescope, which can be represented by the

angular resolution of stellar images blurred by atmospheric turbulence. There are many methods to measure or estimate seeing. A Differential Image Motion Monitor (DIMM) is an instrument used to assess astronomical seeing. Several site testing projects have used it to measure seeing quality. Xinjiang Astronomical Observatory used two DIMMs measuring seeing conditions at the Muztagh-Ata site on the level of ground, 6 and 11 m above the ground. As a comparison, the median seeing at Dome C was estimated to be 0.30 arcsec at 20 m (Ma et al. 2020). DIMMs can directly provide accurate values of seeing. However, a DIMM can only obtain data at the height of the instrument. It is inconvenient and high-cost to investigate the variation of seeing with height. In addition, there are indirect methods to calculate seeing quality. Astronomical seeing was calculated at the surface layer of Dome C, Antarctica with sonic anemometers (Aristidi et al. 2015). Nighttime optical turbulence vertical structure above Dome C was analyzed (Trinquet et al. 2008). This method can gain more variations of seeing with height, but it can only estimate values of the sonic anemometers within the working time range.

Using reanalysis databases is another viable choice to estimate seeing. A reanalysis database is composed of global grid point data obtained by assimilating ground observations, high-altitude observations, satellites and other data. It has

* Corresponding author.

become a major data resource in the field of global climate change and weather forecasting model improvement research. Relying on reanalysis databases to access the quality of atmospheric parameters is widespread all over the world and demonstrated a high level of significance (Hach et al. 2012). Climate Forecast System Reanalysis (CFSR) was used to estimate seeing and other atmospheric parameters in Tibet (Ye et al. 2016). National Centers for Environmental Prediction (NCEP)/ National Centers for Atmospheric Research (NCAR) reanalysis databases were employed to study atmospheric parameters at Oukaimeden Observatory (Bounhir et al. 2009). The European Centre for Medium-Range Weather Forecasts (ECMWF) reanalysis databases have been also widely utilized in atmospheric analysis. The characteristics of optical turbulence over the South China Sea were acquired by analyzing the meteorological data obtained from the field experiment of ocean optical parameters and the ECMWF ERA5 during 2011–2020 (Xu et al. 2022). The cloud cover, vertical integral of mean kinetic energy, inverse values of Richardson number $1/Ri$ and other parameters were analyzed in the Big Telescope Alt-azimuthal (BTA) region from ERA5 (Shikhovtsev et al. 2022). In the Tibetan Plateau, optical turbulence was analyzed using ERA5 data (Han et al. 2021). ECMWF and NCEP were compared all over the world. Climate change in the Tibetan Plateau has been compared and analyzed between NCEP and ECMWF (Li et al. 2004). Reanalysis databases can be employed to derive more information about the long-term evolution of atmospheric parameters including seeing. This method can be used to examine seeing at any height and any time. It is more convenient to analyze the variation of seeing over a wide range of height and time.

Seeing conditions measured at different heights and times at the Muztagh-Ata site are essential for constructing telescopes to estimate the image quality disturbed by atmosphere turbulence. Using reanalysis databases can perfectly meet this requirement. In this paper, we use ERA5 Reanalysis databases to estimate seeing at the Muztagh-Ata site over different heights and times. The paper is organized as follows. The detailed theory of seeing calculation and descriptions and data processing of reanalysis databases and meteorological instruments are presented in Section 2. The analysis and comparisons of seeing conditions are presented in Section 3. The influence of atmospheric turbulence on seeing is discussed in Section 4. Conclusions are provided in Section 5.

2. Data and Method

2.1. ERA5 Reanalysis Databases and Pre-processing

We choose ERA5 Reanalysis because of the free data access, high spatial and temporal resolution and long temporal coverage. ERA5 is the fifth generation ECMWF reanalysis for the global climate and weather from 1940 to present. Reanalysis combines model data with observations from across

the world into a globally complete and consistent data set using the laws of physics. This principle, called data assimilation, is based on the method used by numerical weather prediction centers, where every so many hours (12 hr at ECMWF) a previous forecast is combined with newly available observations in an optimal way to produce a new best estimate of the state of the atmosphere, called analysis, from which an updated, improved forecast is issued. ERA5 provides hourly estimates for a large number of atmospheric, ocean-wave and land-surface quantities (Hersbach et al. 2020). This paper gets variables of hourly temperature, wind and geopotential height above 2 levels which are 550 mbar and 600 mbar at a resolution of $0^\circ.25 \times 0^\circ.25$. The seeing is calculated only when the sky is deemed usable (Ye et al. 2016). Reanalysis databases rely on Coordinated Universal Time (UTC). The time range from 2017 December 31st to 2021 December 31st is used.

To compare reanalysis data with meteorological data and calculate seeing, we have done the following pre-processing:

- (1) The precise horizontal location of the Muztagh-Ata site can be extrapolated through two-dimensional linear interpolation from four adjacent points on the horizontal plane.
- (2) As for vertical coordinates, the geopotential height should be transformed to geometric height first. China reference atmosphere (ground to 80 km) (Li et al. 2007) gives an empirical formula for the transformation. Sea level gravitational acceleration at a given latitude can be computed by

$$g_{0,\varphi} = 9.80616(1 - 0.002637 \cos 2\varphi + 0.0000059 \cos^2 2\varphi), \quad (1)$$

where $g_{0,\varphi}$ is sea level gravitational acceleration (m s^{-2}) and φ is the latitude ($^\circ$). Then the Earth radius calibration value can be computed by

$$r_\varphi = \frac{2g_{0,\varphi}}{3.085462 \times 10^{-6} + 2.27 \times 10^{-9} \cos 2\varphi}, \quad (2)$$

where r_φ is the Earth radius calibration value (m). Combining the above two values, the conversion formula of geopotential height and geometric height can be obtained by

$$h = \frac{r_\varphi \cdot H}{\frac{r_\varphi \cdot g_{0,\varphi}}{g_{np}} - H}, \quad (3)$$

where h is geometric height (m) and H is geopotential height (gpm). $g_{np} = 9.80665$. We focus on the height above ground in this paper, so geometric height needs to subtract the Muztagh-Ata site's altitude for the calculation.

- (3) Using the values of geometric height, meteorological elements can be extrapolated through a simple linear interpolation formula from two adjacent points on the vertical

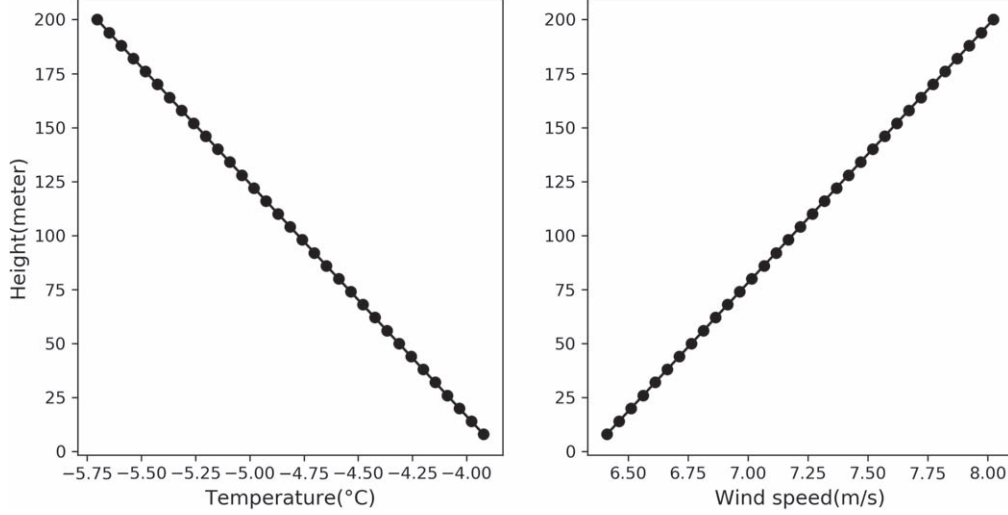


Figure 1. Variations of temperature and wind with height after linear interpolations of the ERA5 Reanalysis database on Oct 5th in 2021.

plane. Figure 1 shows how temperature and wind vary with height after linear interpolations of the ERA5 Reanalysis database on October 5th in 2021.

2.2. Seeing Calculation

Seeing discussed in this article is the astronomical seeing, which is related to the angular resolution of stellar images blurred by atmospheric turbulence. Seeing quality therefore results from an integration along the line of sight of the structure constant of the refractive index C_n^2 . The theoretical basis of the effects of turbulence is described in Roddier (1981).

The temperature structure function indicating the temperature fluctuations at two points separated by a distance ρ is given by

$$D_T^2(\rho) = \langle (T(\mathbf{r}) - T(\mathbf{r} + \rho))^2 \rangle, \quad (4)$$

where \mathbf{r} is the position of one point, T is the temperature and $\langle \rangle$ is average. As our instruments provide data in the form of a time series, we have to transform ρ to $\bar{v}\Delta t$ (\bar{v} is the mean wind and Δt is the time interval between two measurements) as

$$D_T^2(\bar{v}\Delta t) = \langle (T(t) - T(t + \Delta t))^2 \rangle. \quad (5)$$

according to Taylor's hypothesis.

This function behaves as a $\frac{2}{3}$ power law when ρ is between the dynamic inner scale l_0 and the outer scale L_0 . The function tends to be a constant when ρ is outside the above interval. Within the range, the structure constant of the temperature C_T^2 is defined as

$$D_T(\rho) = C_T^2 \rho^{\frac{2}{3}}. \quad (6)$$

Initially, a least-squares fit of a function $C_T^2 \rho^\alpha$ should be performed in the interval $[l_0, L_0]$ (inertial range). The value α

should be around $\frac{2}{3}$. If α deviates too much from $\frac{2}{3}$, it means that the function does not obey the power law. If α is around $\frac{2}{3}$, C_n^2 can be calculated as (Aristidi et al. 2015)

$$C_T^2 = \left\langle \frac{[T(t) - T(t + \delta t)]^2}{[v(t)\delta t]^{\frac{2}{3}}} \right\rangle_\tau. \quad (7)$$

Here $v(t)$ is wind $v(t) = \sqrt{u^2 + v^2 + w^2}$, and u, v, w represent three orthogonal directional components of wind respectively. Then the structure constant of the refractive index C_n^2 can be expressed as

$$C_n^2 = 6.24 \times 10^{-9} C_T^2 P^2 T^{-4}, \quad (8)$$

where temperature T is in kelvin and pressure P in hPa. The seeing ϵ at an altitude h_0 is computed by the following integral over the altitude z as

$$\epsilon = 5.25 \lambda^{-\frac{1}{5}} \left[\int_{h_0}^{\infty} C_n^2(z) dz \right]^{\frac{3}{5}}, \quad (9)$$

where λ is the wavelength which is set to be 500 nm. The variation of $\ln(C_n^2)$ values with height on October 5th (UTC+8) is shown in Figure 2 from the ERA5 Reanalysis. As shown in the figure, C_n^2 exhibits a negative exponential power change with height within the surface layer, which can be fitted as a negative exponential power function to calculate seeing. We use measured values from DIMMs to determine fitting coefficients and rely on these fitting coefficients to infer seeing at any height or time. After power function fitting, we find that the integral converges well to a single value. The seeing calculation method above can be applied to daytime and nighttime. The difference of the heating conditions between daytime and nighttime would not affect the application of this method (Masciadri et al. 2001; Shikhovtsev et al. 2023). The

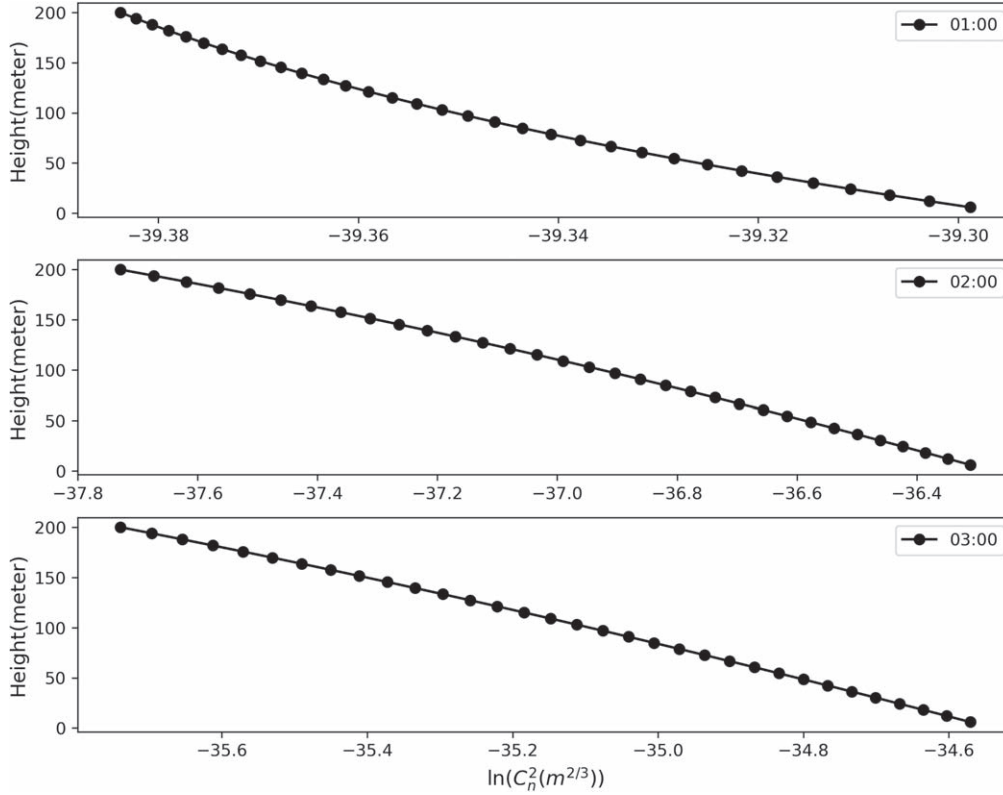


Figure 2. Variation of $\ln(C_n^2)$ values with height on Oct 5th(UTC+8) from ERA5 Reanalysis.

comparisons of seeing between measurements and calculations will be shown in Section 3.2.

3. Results

3.1. Comparisons of Temperature and Wind between ERA5 and Ultrasonic Anemometers

In order to confirm the reliability of ERA5 databases, atmospheric parameters from ERA5 and meteorological data need to be compared. The meteorological data are provided by Xinjiang Astronomical Observatory. Temperature and wind are from a set of ultrasonic anemometers installed on a 30 m tower. Five ultrasonic anemometers were installed at the heights of 6 m, 12 m, 18 m, 24 m and 30 m above the ground on the tower. The data cover one month, from 2021 October 1st to 2021 October 31st. The sign of the wind represents the wind direction; $+u$ values mean wind from the east, $+v$ values signify wind from the north and $+w$ values correspond to wind from below. The two elements were provided at a rate of 20 Hz.

To derive seeing, the structure constant C_n^2 should be derived first, which comes after the estimation of the structure function $D_T^2(\rho)$. As the rate of ultrasonic anemometer is 20 Hz, we set δt as a 0–168 array with gradient of 12 in Equation (5) after some trials. The temporal average has to be calculated on a time

interval τ in Equation (7) long enough to ensure statistical significance and shorter than the characteristic time of evolution of C_n^2 . It is found that $\tau = 1$ hr is a good compromise because we need data size matching seeing from reanalysis data, which means we need to get the average seeing of one hour. In Equation (8) we take T for the average temperature over 1 minute, and P the mean yearly pressure of the site (586.1 hPa) (Xu et al. 2020a).

The parameters measured are temperature and wind. Daily variations in the temperature and wind in 2021 October with the ultrasonic anemometers are presented in Figure 3 (squares and asterisks). In the same figure, the parameters from ERA5 Reanalysis data are plotted from the same time period (circles). As little difference is shown between two levels from both databases, only two levels (12 and 30 m) from ultrasonic anemometers and one level (30 m) from ERA5 are presented in Figure 3(a) and (b). To evaluate the quality of ERA5 Reanalysis, two scores are used: (i) the mean absolute error (MAE); (ii) the standard deviation of the error (standard deviation of the differences between the reanalysis and measurements [STDE]). Results are displayed in Table 1. Both MAE and STDE are small values, which can be interpreted as systematic errors. These differences are acceptable, and the variations and numerical values of temperature and wind

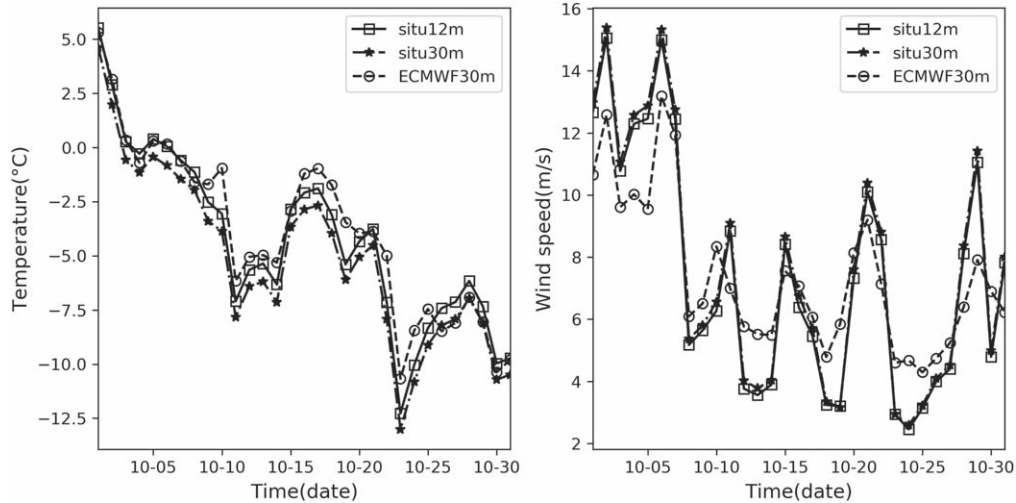


Figure 3. Daily variations of the temperature (a) and wind (b) in 2021 October with the ultrasonic anemometers and ERA5 Reanalysis database at 12 m (squares) and 30 m (asterisks and circles). Circles indicate data from the ERA5 Reanalysis database and squares signify data from ultrasonic anemometers.

Table 1

Mean Values of MAE and STDE in October between ERA5 and In Situ Measurement

Height(m)	6 m	12 m	18 m	24 m	30 m
Temperature MAE(K)	1.54	1.32	1.39	1.40	1.54
Temperature STDE(K)	0.94	0.89	0.93	0.95	1.03
Wind MAE(m s ⁻¹)	2.43	2.48	2.49	2.48	2.47
Wind STDE(m s ⁻¹)	1.79	1.90	1.92	1.93	1.93

between the reanalysis database and in situ measurements are consistent, therefore, we can be confident with the ERA5 database since at 5 levels it has good agreement with in situ measurement. The ERA5 database can be used to determine the temperature and wind at any height or time at the Muztagh-Ata site.

3.2. Comparisons of Seeing Between ERA5 and DIMMs

Seeing values from ERA5 are compared with DIMMs so as to demonstrate the feasibility of the seeing calculation method. The time series of seeing from DIMM were from 01:00 to 06:00 (UTC+8) on Oct 5th of 2021. The DIMM was installed 500 m away from the gradient tower and the height of the DIMM was 6 m. Since the fitting coefficient α from Equation (6) deviates too much from $\frac{2}{3}$ from 04:00 to 06:00 on Oct 5th ($\alpha = 0.28$ from 04:00 to 05:00 and $\alpha = 0.10$ from 05:00 to 06:00), seeing is compared between ERA5 and DIMM from 01:00 to 04:00.

Using Equation (9) the values of seeing quality can be calculated. Figure 4 shows monthly variations of seeing in 2018 at 11 m. Red represents ERA5 values and black signifies those from DIMM (Xu et al. 2020b). Table 2 displays seeing

from ERA5 and DIMM on 5th in October of 2021. There exist small differences due to distance error and error of the fitting function in calculation. Another reason is the 500 m distance between the site location and DIMMs. In general, estimations from ERA5 are consistent with the DIMM values, therefore ERA5 can be used to estimate seeing at any time or height.

3.3. Variations of Seeing

3.3.1. Height Variations

Seeing variations with height in 2021 from ERA5 are shown in Figure 5. From the figure, it can be observed that the seeing decays exponentially with height. Both nighttime and daytime variations of seeing are estimated. To better distinguish the difference in seeing between daytime and nighttime, we divide one day into two parts. As the sunrise time in October at Muztagh-Ata site is about 9 a.m. and the sunset time is about 8 p.m., we define the daytime from 9 a.m. to 8 p.m., and nighttime the remaining hours of a day. According to Ma et al. (2020), the yearly median seeing value at Dome A is 0.31 arcsec at 20 m during the polar night. If we want to achieve the same seeing quality as Dome A at the Muztagh-Ata site, the altitude should be about 100 m at night in fall (September, October, and November) and about 120 m in spring (March, April, and May) and winter (December, January, and February). The difference is caused by topographical reasons. Sites on the Antarctic plateau are characterized by comparatively weak turbulence in the free atmosphere above a strong but thin boundary layer (Ma et al. 2020) while Muztagh-Ata is located in the inland high-altitude area, and the topographical environment of mountainous areas is relatively more complex than that of the Antarctic plateau. Therefore, seeing at the Muztagh-Ata site is higher than at Dome A.

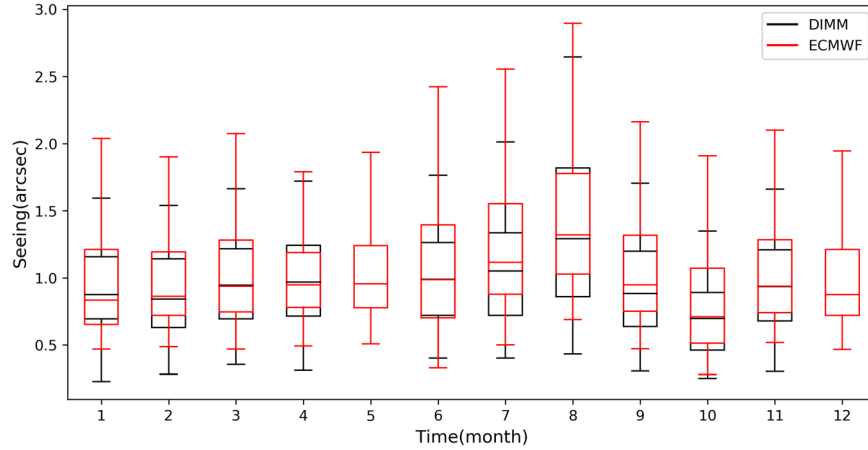


Figure 4. Monthly variations of seeing in 2018. Red represents ERA5 calculation, and black signifies DIMM values. Each box represents the values in the range of 25%–75% and the vertical line signifies the maximum and minimum values, while the horizontal lines inside every box correspond to median values.

Table 2

Seeing from ERA5 and DIMM on 5th in October of 2021(UTC+8)

Seeings(arcsec)	01:00–02:00	02:00–03:00	03:00–04:00
ERA5	0.77	0.82	0.88
DIMM Median	0.79	0.80	0.89
DIMM Range	0.64-0.98	0.68-1.07	0.73-1.13

From Figure 5 we can ascertain that seeing decays the fastest in fall and most slowly with height in spring, perhaps because atmospheric turbulence at high altitude in spring is more active than in fall. At high altitude, seeing is best in fall and worst in summer (June, July and August), probably due to the different conditions of atmospheric layers between fall and summer. At nighttime, seeing is good in winter and fall, indicating the relatively stable atmosphere in winter and fall at night.

3.3.2. Monthly Variations

As the telescopes are installed at a certain height (12 m for MOST), using this method can help us calculate seeing at any height to meet with our needs. We then calculate seeing at 12 m which is a planned telescope construction height using the ERA5 Reanalysis database. The variations of seeing at the Muztagh-Ata site calculated from ERA5 at 12 m were analyzed in 2021. Figure 6(a) depicts the monthly variations of the median seeing at 12 m. The median value of seeing at 12 m is 0.89 arcsec, the maximum value is 1.21 arcsec in August and the minimum value is 0.66 arcsec in October. Significant monthly variations of seeing affirm that the seeing condition is better in fall than in summer. Seeing values between daytime and nighttime have a clear difference. In Figure 6(a), the blue line indicates daytime values and the red line signifies nighttime values in 2021. The median value of seeing at

12 m is 0.72 arcsec in the nighttime and 1.08 arcsec in the daytime. Seeing varies from 0.55 arcsec to 0.98 arcsec during the nighttime and from 0.80 arcsec to 1.47 arcsec during the daytime. Nighttime values are lower than daytime values which is because the atmosphere is relatively stable at night. Overall, daytime, nighttime and all-day trends of seeing are consistent in 2021. Yearly differences are depicted in Figure 6(a). Seeing value in February is a wave crest in 2021 but a wave trough in 2018 (gray dashed line). The maximum and minimum values are in August and October respectively, but seeing is bigger in August in 2018 than in 2021. Moreover, the median value of seeing in 2021 (0.89 arcsec) is smaller than in 2018 (0.96 arcsec).

So as to study deeply the influencing factors of seeing variations with time, monthly variations of temperature and wind are presented. Figure 6(b) and (c) shows the monthly variations of the mean temperature and wind at 12 m in 2021. When the temperature is low, the atmospheric turbulence is generally weak, and the seeing is good, and when the temperature is high, atmospheric turbulence is relatively active, which will seriously affect seeing quality. In Figure 6, black dash-dotted lines refer to the fitting curves. Significant annual variation of temperature and about biannual variation of wind speed are shown. The superposition of an annual variation and a biannual variation is utilized to perform a second harmonic fitting on the variables of seeing, temperature and wind speed. In the case of temperature, where the amplitude of the biannual variation (1.58 °C) is significantly smaller compared to the annual variation (8.33 °C), it can be approximated that temperature is primarily influenced by the annual variation. The annual harmonics of temperature reach their peak around July, while wind speed exhibits its minimum during that period. Similarly, the annual harmonic of seeing reaches its maximum around July and August. Consequently, as both

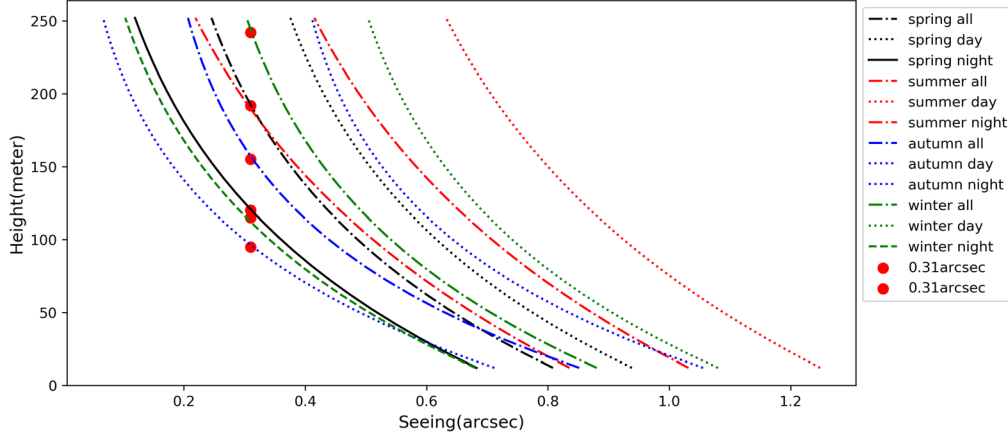


Figure 5. Seeing variations with height in 2021 from ERA5.

temperature and seeing reach their maximum values simultaneously with the same periodicity (annual), there exists a positive correlation between temperature and seeing. Regarding the biannual variations, the harmonic of temperature reaches its maximum around February and August, whereas the harmonic of wind speed peaks around March and September. Additionally, the biannual variation of seeing also reaches its maximums during February and August. The phases of the harmonics for seeing, temperature and wind speed are nearly identical. This suggests that the temporal variation of seeing is influenced by both temperature and wind speed.

4. Discussions

To study the effect of atmospheric turbulence on seeing at different height levels, we define $\Delta\epsilon$ as seeing between two heights. For example, $\Delta\epsilon$ in 6–12 m means integrating Equation (9) from 6 to 12 m. In Figure 7(a), $\Delta\epsilon$ values at different levels from an ultrasonic anemometer in October of 2021 are shown. $\Delta\epsilon$ is smallest at 6–12 m, second smallest at 18–24 m, second biggest at 12–18 m and biggest in 24–30 m. This result might be related with the effect of atmospheric turbulence. Vertical temperature differences corresponding to atmospheric turbulence reveal a strong relationship with seeing (Marks et al. 1996). Further, the regions where turbulence occurs and dynamic and static stability have been estimated. Under a temperature inversion condition, the Richardson number (Ri) can quantify stability. Following Mahrt & Vickers (2006), Ri between two levels can be calculated as

$$Ri = \frac{g}{\theta_0} \frac{d\theta/dz}{(dV/dz)^2}, \quad (10)$$

where g is the acceleration of gravity, z is height above the surface, V is the wind speed, θ is the potential temperature in K, and θ_0 is the average value between two levels. Richardson number represents the effects of temperature stratification and

wind shear on turbulence. The numerator part of Ri is a criterion for static stability and the denominator represents dynamic stability. If $Ri < 0$, it indicates an unstable temperature stratification. According to Liu et al. (1988), $Ri < 0.25$, which means the vertical wind shear phase is more than four times smaller than the vertical temperature difference, is a necessary condition for the occurrence of turbulence. If $Ri > 0.25$, it indicates stable temperature stratification. The ratio of $Ri < 0$, $0 < Ri < 0.25$ and $Ri > 0.25$ has been considered to learn about the temperature stratification condition. In Figure 7(b), the ratio of Ri from and ultrasonic anemometer in October 2021 is shown. All $Ri < 0$ at 24–30 m, indicating an unstable temperature stratification. At 6–12 m, the value of $Ri < 0$ is smallest, indicating the temperature stratification is relatively stable. The proportion of $Ri > 0.25$ is biggest (81.7%) at 6–12 m and second biggest (36.0%) at 18–24 m in the nighttime. That is, dynamic stability is best at 6–12 m and second best at 18–24 m. Therefore, the probability of the occurrence of turbulence is smallest at 6–12 m and second smallest at 18–24 m. The above results of Ri match with $\Delta\epsilon$ well. In summary, Ri can be used to analyze the atmospheric stability between layers, so as to further analyze the quality of seeing.

5. Conclusions

ERA5 is used to quantitatively estimate seeing at the Muztagh-Ata site. The variations of seeing with height and time are analyzed. The main results are as follows:

- (1) The temperature and wind from ERA5 are compared with ERA5 and ultrasonic anemometers, which show consistent variations, indicating the reliability of the ERA5. Seeing from ERA5 is consistent with DIMMs at 6 m and 11 m, confirming the feasibility of the calculation method based on the effects of turbulence.

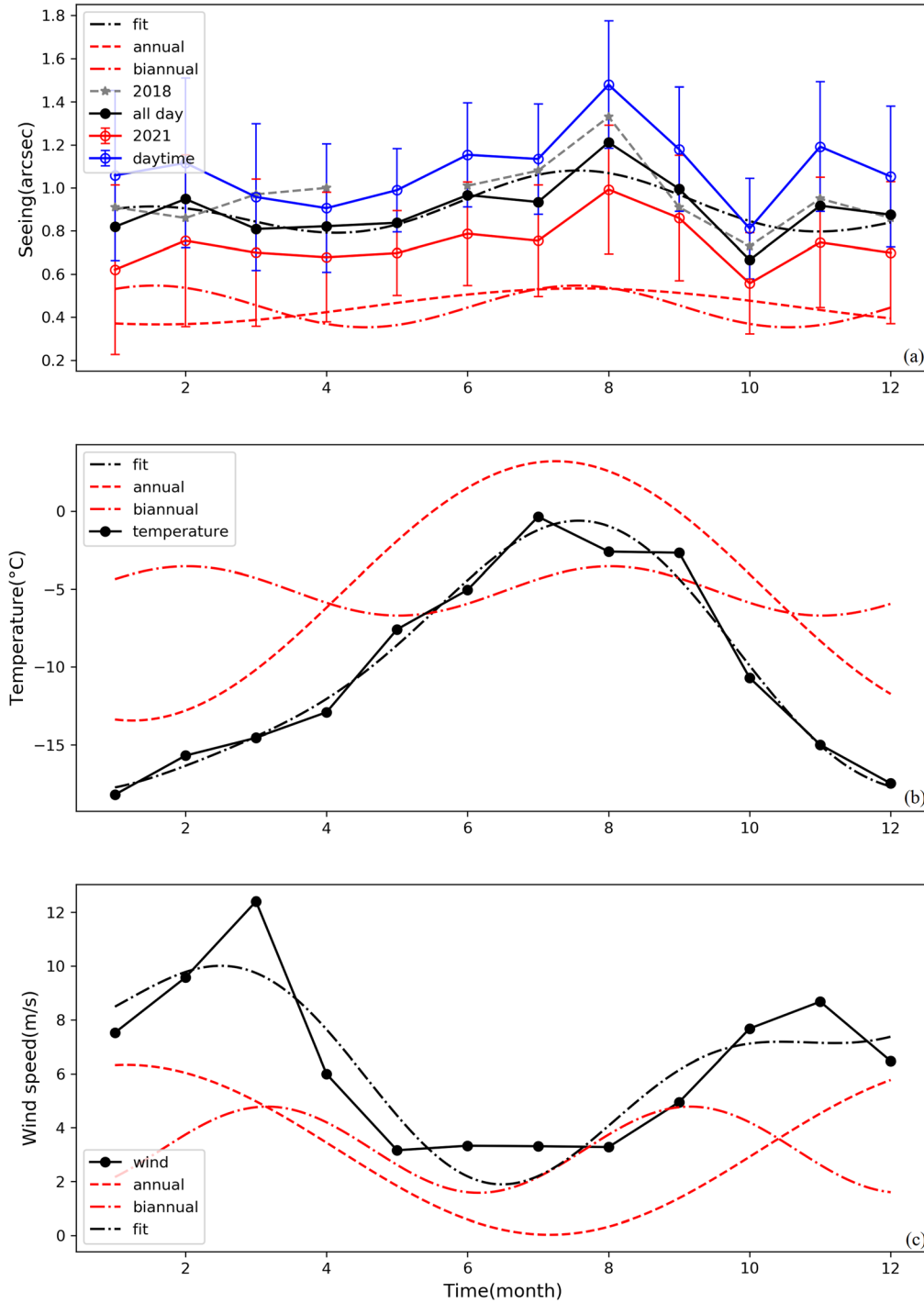


Figure 6. (a) Monthly variations of the median seeing (black) at the level of 12 m in 2021. (b) Monthly variations of mean temperature at 12 m in 2021. (c) Monthly variations of mean wind at 12 m in 2021.

(2) Seeing decays exponentially with height at the Muztagh-Ata site. If we want to achieve the same seeing quality as Dome A at the Muztagh-Ata site, the altitude should be about 100 m at night in fall. Seeing decays the fastest in

fall and most slowly with height in summer. Above 50 m, seeing is best in fall and worst in summer.
 (3) The seasonal variations of seeing at the Muztagh-Ata site calculated from ERA5 at 12 m are analyzed in 2021. A

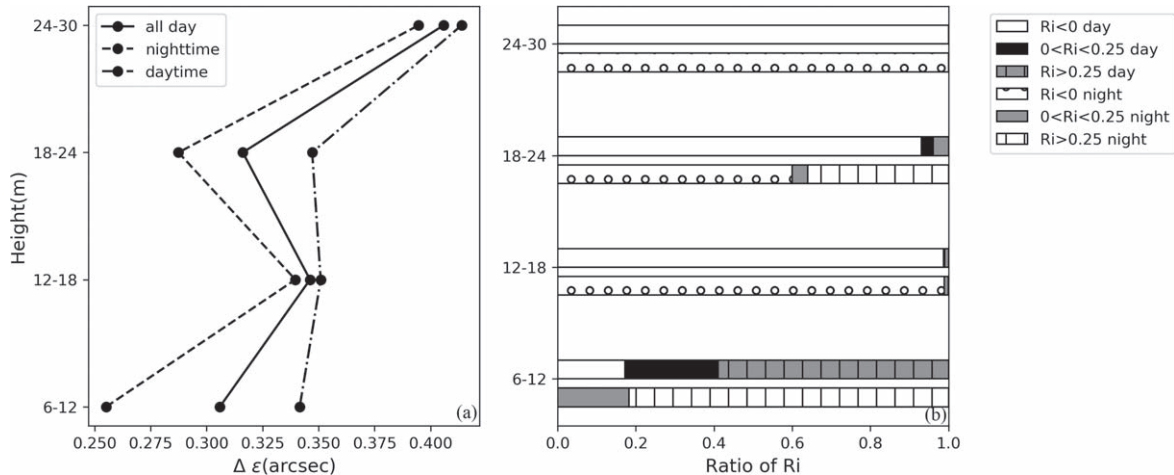


Figure 7. (a) $\Delta\epsilon$ at different levels from an ultrasonic anemometer in October of 2021. Dash-dotted line indicates daytime values and dashed line signifies nighttime values. (b) Ratio of Ri from ultrasonic anemometer in October of 2021.

strong correlation of temperature and a small adjustment effect of wind speed on seeing are shown. The median value of seeing at 12 m is 0.89 arcsec, the maximum value is 1.21 arcsec in August and the minimum value is 0.66 arcsec in October. Significant monthly variations of seeing are apparent such that the seeing condition is better in fall than in summer. The median value of seeing is 0.72 arcsec in the nighttime and 1.08 arcsec in the daytime.

- (4) Seeing is a combination of annual and about biannual variations with the same phase as temperature and wind speed. Seeing variation with time is influenced by temperature and wind speed. Seeing variations with height can be explained by the atmospheric stability between different layers. The results of Ri are consistent with the quality of seeing between different layers.

These results can be used in a telescopic observation strategy and in estimating the quality of an observed image. For further development, based on a reanalysis database, seeing measured by DIMMs, temperature and wind measured by ultrasonic anemometers at the Muztagh-Ata site could be assimilated into a numerical model called WRF, gaining a more reliable assimilation of data used to analyze the variations of seeing.

Acknowledgments

We thank the ERA5 Reanalysis data provided by the ECMWF, from their website: <https://cds.climate.copernicus.eu/cdsapp#!/dataset/10.24381/cds.bd0915c6?tab=overview>. This work is funded by the National Natural Science Foundation of China (NSFC) and the Chinese Academy of Sciences (CAS) (grant No. U2031209), the National Natural

Science Foundation of China (NSFC, grant Nos. 11872128, 42174192, and 91952111).

ORCID iDs

Xiao-Qi Wu <https://orcid.org/0000-0001-5598-5335>

Cun-Ying Xiao <https://orcid.org/0000-0002-6742-8269>

References

- Aristidi, E., Vernin, J., Fossat, E., et al. 2015, *MNRAS*, **454**, 4304
 Bounhir, A., Benkhaldoun, Z., Carrasco, E., & Sarazin, M. 2009, *MNRAS*, **398**, 862
 Feng, L., Hao, J.-X., Cao, Z.-H., et al. 2020, *RAA*, **20**, 080
 Hach, Y., Jabiri, A., Ziad, A., et al. 2012, *MNRAS*, **420**, 637
 Han, Y.-J., Yang, Q.-K., Liu, N.-N., et al. 2021, *MNRAS*, **501**, 4692
 Hersbach, H., Bell, B., Berrisford, P., et al. 2020, *QJRMS*, **146**, 1999
 Li, C., Zhang, Y.-J., & Chen, J. 2004, *Plateau Meteorology*, **023**, 97
 Li, Q., Xie, Z.-H., Yan, S.-Y., et al. 2007, in *Standardization Administration of the People's Republic of China, China Reference Atmosphere (ground 80 km)*, ed. R.-P. Ma et al. (Beijing: GJB 5601-2006)
 Liu, S.-D., Pan, N.-X., & Chen, J.-Y. 1988, *AtSc*, **12**, 1
 Ma, B., Shang, Z.-H., Hu, Y., et al. 2020, *Nature*, **583**, 771
 Mahrt, L., & Vickers, D. 2006, *BoLMc*, **119**, 19
 Marks, R. D., Vernin, J., Azouit, M., et al. 1996, *A&AS*, **118**, 385
 Masciadri, E., Vernin, J., & Bougeault, P. 2001, *A&A*, **365**, 699
 Roddier, F. 1981, *Progress in Optics*, Vol. 19 (Amsterdam: Elsevier), 281
 Shi, S.-C., Paine, S., Yao, Q.-J., et al. 2016, *NatAs*, **1**, 1
 Shikhovtsev, A. Y., Kovadlo, P. G., Khaikin, V. B., et al. 2022, *RemS*, **14**, 1833
 Shikhovtsev, A. Y., Kovadlo, P. G., Lezhenin, A. A., et al. 2023, *Appl. Sci.*, **13**, 6354
 Trinquet, H., Agabi, A., Vernin, J., et al. 2008, *PASP*, **120**, 203
 Xu, J., Esamdin, A., Hao, J.-X., et al. 2020a, *RAA*, **20**, 086
 Xu, J., Esamdin, A., Hao, J.-X., et al. 2020b, *RAA*, **20**, 087
 Xu, M.-M., Shao, S.-W., Weng, N.-Q., & Liu, Q. 2022, *RemS*, **14**, 4398
 Ye, Q.-Z., Su, M., Li, H., & Zhang, X.-M. 2016, *MNRAS: Letters*, **457**, 1
 Zhou, X., Wu, Z. Y., Jiang, Z. J., et al. 2010, *RAA*, **10**, 279